

# Wave Transition and Trapping by Suddenly Created Periodic Plasma

Spencer P. Kuo\*

**Abstract**—Theory, numerical simulation, and experiment on the interaction of electromagnetic wave with suddenly created periodic plasma layers are presented. In the experiment, frequency-downshifted signals of considerably large spectral width and enhanced spectral intensity were detected. Numerical simulation of the experiment, that the plasma has a finite periodic structure and is created much faster than its decay, shows that the frequency downshifted waves have a broad power spectrum and are trapped in this plasma crystal until the plasma frequency drops to become less than the wave frequency. The spectral power increases exponentially with the frequency of the frequency downshifted wave, consistent with the experiment. The simulation reveals that wave trapping results in accumulating the frequency-downshifted waves generated in the finite transition period of plasma creation and decay. Though frequency-upshifted signals were missing in the experimental measurement, it might be attributed to the collision damping of the plasma.

## 1. INTRODUCTION

The space-time duality indicates that some analogies between phenomena of electromagnetic wave propagation in spatially varying and in time varying media may be drawn straightforwardly [1, 2]. It is indeed so for many of those, but some fundamental differences also exist. For example, the causality concept forbids the time domain reflection phenomenon, the sharp discontinuity in the spatial domain does not exist in reality in the time domain, and most significantly, wave can pre-exist in a time varying medium but it has to propagate into a spatially varying medium.

Jiang [3] and Wilks et al. [4] studied the wave propagation in instantly generated uniform plasma. They find that the wavelength stays fixed, the frequency is upshifted and the initially forward propagating wave splits into a forward and a backward propagating component at a higher frequency. A new phenomenon, which is not foreseen by the duality, is the generation of a static wiggler magnetic field having the same wavelength as that of the original wave. Theory has been extended to consider wave propagation in rapidly created plasma slab [5, 6]. As the transition period of the medium (e.g., finite creation time of the plasma) increases, it is shown numerically that the frequency spectra of the frequency-upshifted waves are broadened [4, 5]. Consequently, the wavenumber spectra of these waves after propagating out of the plasma slab are also broadened, unlike the spatial domain phenomenon that the wavenumber spectrum of the wave will not be broadened after transmitting a pre-exist plasma slab.

Experiments of wave interaction with rapidly created plasmas have been performed to demonstrate the frequency upshifting and spectral broadening phenomena [7–13]. In the pulse propagation experiments, frequency upshift by pulse-induced plasma was observed; but unexpected frequency downshifted spectral lines were also recorded in the measurements. These lines together with those of frequency upshifted led to the spectral breaking of the pulse spectrum [14]. It was verified that the damping of the pulse by the plasma in the transition period was responsible for the frequency downshifting result [14].

---

*Received 6 July 2014, Accepted 14 August 2014, Scheduled 22 August 2014*

\* Corresponding author: Spencer P. Kuo (skuo@poly.edu).

The author is with the Department of Electrical & Computer Engineering, Polytechnic School of Engineering, New York University, 5 MetroTech Center, Brooklyn, NY 11201, USA.

A spatially periodic dielectric medium supports discrete branches of Floquet modes [15–17]. A time harmonic incident electromagnetic wave is scattered into this medium to its Floquet modes of different wavelengths [17, 18]. On the other hand, if this medium such as a plasma is created suddenly in time, rather than preexisting in space, one would expect that the temporal transition and spatial periodic structure of the plasma would convert the original wave to Floquet modes of this plasma at different frequencies [16], which include upshifted frequencies greater than that by a single suddenly created plasma slab of the same plasma density as well as downshifted frequency in the cutoff region of a single plasma slab. This was investigated experimentally.

In the experiment, spatially periodic plasma was generated by the electric discharge of a set of evenly separated parallel plate pairs; the plasma frequency was time dependent. Plasma first increased rapidly and then decayed, with the time scales not necessarily short compared with the wave period. The frequency downshifted waves have indeed been observed in the experiment; however, the frequency upshifted waves were missing (i.e., they could not be distinguished conclusively from the noise). Moreover, the spectral intensity and width of the frequency downshifted waves were found to be unexpectedly high and wide. The experimental result was understood via the numerical simulation which indicated that the periodic structure could trap the frequency downshifted waves. The accumulation of the frequency downshifted waves during the transition period led to the significant enhancement of the spectral intensity (20 to 50 dB above the noise level) and the spectral width.

In Section 2, theory of up-shifting electromagnetic wave frequency by instantly created uniform plasma is presented. The theory is extended to an instantly created spatially periodic plasma distribution; the formulation and analysis are presented in Section 3. The experiment and numerical simulation of frequency shift and wave trapping by rapidly created periodic plasma are compared and presented in Section 4. A summary is given in Section 5.

## 2. INTERACTION OF WAVE WITH SUDDENLY CREATED PLASMA

In unmagnetized plasma which varies arbitrarily in space and time, the wave equation is given by

$$[\partial_z^2 - c^{-2}\partial_t^2 - \omega_p^2(z, t)/c^2] \varepsilon(z, t) = 0 \quad (1)$$

where  $\omega_p(z, t) = [N_0(z, t)e^2/m_e\varepsilon_0]^{1/2}$  is the electron plasma frequency,  $N_0$  is the electron density,  $e$  is the magnitude of the electron charge,  $m_e$  is the electron mass, and  $\varepsilon_0$  is the permittivity of the free space. If the plasma is uniform in space and stationary in time, i.e.,  $N_0$  is a constant, the dispersion relation of the electromagnetic (EM) mode of the plasma is obtained from (1) to be  $\omega = (\omega_p^2 + k^2c^2)^{1/2}$ . We now study the propagation of a plane wave when uniform plasma is suddenly created in the background. Prior to the plasma creation at  $t = 0$ , the wave fields of this plane wave propagating in the free space are

$$\varepsilon(z, t \leq 0) = \hat{\mathbf{x}}E_0 \cos(k_0z - \omega_0t) \quad \text{and} \quad \mathbf{h}(z, t \leq 0) = \hat{\mathbf{y}}(E_0/\eta_0) \cos(k_0z - \omega_0t) \quad (2)$$

where  $k_0 = \omega_0/c$  is the wavenumber and  $\eta_0 = (\mu_0/\varepsilon_0)^{1/2}$  is the intrinsic impedance of the free space. After a uniform plasma is suddenly created with  $\omega_p^2(z, t > 0) = \omega_p^2 = \text{const.}$  at  $t = 0$ , the wave fields (2) are not the solution of the wave Equation (1) anymore; but the wavelength  $\lambda_0$  of the wave and the spatial distributions of the wave fields remain unchanged in the transition of the background, i.e.,

$$\varepsilon(z, t = 0^+) = \varepsilon(z, t = 0^-) = E_0 \cos k_0z \quad (3a)$$

and

$$h(z, t = 0^+) = h(z, t = 0^-) = (E_0/\eta_0) \cos k_0z \quad (3b)$$

These in (3) serve as the initial conditions of Equation (1). The wave propagation in plasma follows the dispersion relation  $\omega = (\omega_p^2 + k_0^2c^2)^{1/2}$ , as a result the frequency of the wave has to be upshifted to  $\omega = (\omega_p^2 + \omega_0^2)^{1/2}$ . Thus the solution of (1) in  $t > 0$  can be introduced to be

$$\varepsilon(z, t > 0) = \hat{\mathbf{x}}[A_+ \cos(k_0z - \omega t) + A_- \cos(k_0z + \omega t)] \quad (4)$$

where

$$A_+ + A_- = E_0 \quad (5)$$

so that (4) satisfies the initial condition (3a).

From Faraday's Law  $\nabla \times \boldsymbol{\varepsilon} = -\mu_0 \partial_t \mathbf{h}$ , the corresponding wave magnetic field  $\mathbf{h}$  is obtained to be

$$\mathbf{h}(z, t > 0) = \hat{\mathbf{y}}(k_0/\mu_0\omega) [A_+ \cos(k_0z - \omega t) - A_- \cos(k_0z + \omega t)] + \mathbf{h}_w(z) \quad (6)$$

where  $\mathbf{h}_w(z)$  is a static field. With the aid of the initial condition (3b), this static field is determined to be

$$\mathbf{h}_w(z) = \hat{\mathbf{y}}(k_0/\mu_0\omega) [(\omega/\omega_0)E_0 - (A_+ - A_-)] \cos k_0z \quad (7)$$

This is a wiggler magnetic field generated together with the frequency upshifted waves in this instantly created plasma.

A space charge current density,  $\mathbf{j} = -eN_0\mathbf{v}_e$ , associated with the fields (4) and (6) will be induced in plasma. Their relationship is governed by the Ampere's law,  $\mathbf{j} = -\varepsilon_0 \partial_t \boldsymbol{\varepsilon} + \nabla \times \mathbf{h}$ . Although plasma is conducting, it takes time for plasma to response to the wave fields. At  $t = 0^+$ , plasma is just created and there was no time for plasma to response to the wave fields, i.e., the velocity response  $v_e(z, t = 0^+) = 0$ . Thus, at  $t = 0^+$ ,  $\mathbf{j} = 0$  and  $\nabla \times \mathbf{h} = \varepsilon_0 \partial_t \boldsymbol{\varepsilon}$  which yields

$$A_+ - A_- = (\omega_0/\omega)E_0 \quad (8)$$

The product of (5) and (8) gives  $\omega_0 E_0^2 = \omega(A_+^2 - A_-^2)$ , an adiabatic invariant. The relations (5) and (8) give  $A_+ = (1 + \omega_0/\omega)E_0/2$  and  $A_- = (1 - \omega_0/\omega)E_0/2$ , which comply with the conservation of momentum. The momentum density  $\mathbf{P}$  of the wave is given by  $\mathbf{P} = \mathbf{S}/v_g^2$ , where  $\mathbf{S} = \boldsymbol{\varepsilon} \times \mathbf{h}$  is the Poynting vector and  $v_g = \partial\omega/\partial k$  is the group velocity. At  $t = 0^-$ ,  $v_g = c$  and  $\mathbf{S}_< = \hat{\mathbf{z}}(E_0^2/\eta_0) \cos^2 k_0z$ , giving  $\mathbf{P}_< = \hat{\mathbf{z}}(E_0^2/\eta_0 c^2) \cos^2 k_0z$ ; at  $t = 0^+$ ,  $v_g = (\omega_0/\omega)c$  and  $\mathbf{S}_> = \hat{\mathbf{z}}(k_0/\mu_0\omega)(A_+^2 - A_-^2) \cos^2 k_0z$ , thus  $\mathbf{P}_> = \hat{\mathbf{z}}(\omega/\omega_0\eta_0 c^2)(A_+^2 - A_-^2) \cos^2 k_0z = \hat{\mathbf{z}}(E_0^2/\eta_0 c^2) \cos^2 k_0z = \mathbf{P}_<$ .

The power conversion ratios to forward and backward frequency upshifted waves are  $\Gamma^+ = (\omega_0/\omega)(1 + \omega_0/\omega)^2/4$  and  $\Gamma^- = (\omega_0/\omega)(1 - \omega_0/\omega)^2/4$ , respectively. Some of the wave energy is converted to the energy of the wiggler magnetic field (7). The amount of frequency upshift is given by  $\Delta\omega = (\omega_p^2 + \omega_0^2)^{1/2} - \omega_0 \cong \omega_p^2/2\omega_0$  for  $\omega_p^2 \ll \omega_0^2$ , and  $\cong \omega_p$  for  $\omega_p^2 \gg \omega_0^2$ . However, the power conversion efficiencies of frequency upshifted waves decrease as the frequency upshift increases.

### 3. SPATIALLY PERIODIC PLASMA

A wave interacts with suddenly created uniform plasma, its frequency is upshifted; this wave is not trapped in the plasma. On the other hand, if plasma is created with a spatially periodic feature, the wave is expected to be converted to Floquet modes, which include frequency upshifted and downshifted and the frequency downshifted mode may be trapped in plasma. Consider that plasma is created rapidly at  $t = 0$  with a spatially periodic structure in the form of parallel slabs and has the plasma frequency

$$\omega_p^2(z, t) = 0 \quad \text{for } t < 0 \quad (9a)$$

and

$$\omega_p^2(z, t) = \omega_{p0}^2 [1 - \exp(-t/\tau_r)] \exp(-t/\tau_d) \sum_{n=0}^{N-1} P_{d/2}(z - nL - L/2) \quad \text{for } t > 0 \quad (9b)$$

where  $\tau_r$  and  $\tau_d$  are the plasma rise and decay times respectively, with  $\tau_d \gg \tau_r$ ;  $P_{d/2}(z - a)$  is a unit rectangular pulse of width  $d$  centered about  $z = a$ ,  $L$  is the separation between two adjacent slabs with  $L \geq d$ , the thickness of each plasma slab, and  $N$  is the total number of plasma slabs in the structure. If  $N$  in (9) is rather large, this plasma can be considered as a periodic dielectric medium which is characterized by the Floquet modes. In the following the dispersion equation for the Floquet modes of an ideal periodic plasma, which is created instantly and does not decay, is derived and analyzed.

#### 3.1. Modes of One-Dimensional Periodic Plasma

We now set the index  $n$  of the summation to run from  $-\infty$  to  $\infty$ , the rise time  $\tau_r \rightarrow 0$ , and the decay time  $\tau_d \rightarrow \infty$  in (9b), and analyze the EM modes in such a periodic plasma with

$\omega_p^2(z, t) = \omega_{p0}^2 \sum_{n=-\infty}^{\infty} P_{d/2}(z - nL - L/2)$ . Assume  $\exp(-i\omega t)$  time dependence, the phasor solution of (1) in one spatial period  $-\ell < z < \ell + d$ , where  $\ell = (L - d)/2$ , can be written as

$$E(z) = \begin{cases} (A \exp(ikz) + B \exp(-ikz), & -\ell < z < \ell \\ C \exp[ikn(z - \ell)] + D \exp[-ikn(z - \ell)], & \ell < z < \ell + d \end{cases} \quad (10)$$

where  $k = \omega/c$  and  $n = (1 - \omega_{p0}^2/\omega^2)^{1/2}$  are the free space wavenumber and the index of refraction of the plasma slab, respectively. Applying the boundary conditions at  $z = \pm\ell : E(\pm\ell_-) = E(\pm\ell_+)$  and  $\partial_z E(\pm\ell_-) = \partial_z E(\pm\ell_+)$  and using the Block wave condition:

$$E(z) = \exp(-i\beta L)E(z + L) \quad (11)$$

to replace  $E(-\ell_-)$  by  $e^{-i\beta L}E[(\ell + d)_-]$ , where  $E[(\ell + d)_-]$  is given by (10) and  $\beta$  is the propagation constant for the periodic structure as a whole, four algebraic equations are obtained. Three of them can be solved to express  $B, C, D$  in terms of  $A$  as follows:

$$\begin{aligned} B &= - \left[ b - (b^2 - 1)^{1/2} \right] A \\ C &= (1/2n) \left\{ (n + 1) \exp(ik\ell) - (n - 1) \left[ b - (b^2 - 1)^{1/2} \right] \exp(-ik\ell) \right\} A \\ D &= (1/2n) \left\{ (n - 1) \exp(ik\ell) - (n + 1) \left[ b - (b^2 - 1)^{1/2} \right]^{1/2} \exp(-ik\ell) \right\} A \end{aligned} \quad (12)$$

where  $b = [(1 + n^2) \cos 2k\ell + 2ncot(knd) \sin 2k\ell]/(n^2 - 1)$ . Substitute (12) into the fourth algebraic equation, results to the dispersion equation

$$\cos \beta L = \cos(knd) \cos 2k\ell - [(n^2 + 1)/2n] \sin(knd) \sin 2k\ell \quad (13)$$

Since  $\cos \beta L$  is an even periodic function, (13) has to be solved only for  $0 \leq \beta L \leq \pi$ . Let  $\varepsilon(z, t = 0^-) = E_0 \cos k_0 z$ , this field distribution does not change at  $t = 0^+$ , i.e.,  $\varepsilon(z, t = 0^+) = E_0 \cos k_0 z$ , because the plasma is created instantly. The phasor of this field is given by  $E(z) = E_0 \exp(ik_0 z)$ . Substitute this phasor function into the Block wave condition (11), yields the relation  $\beta - k_0 = -2\pi/L$ .

Equation (13) has multiple roots,  $\omega_j(\beta)$ ,  $j = 1, 2, \dots$ , each root contributes to a branch of modes and covers a frequency range as a pass band. The dispersion curves of the branches  $\omega_j(\beta)$  form a band diagram similar to that for electron waves in solids [19]. This band diagram identifies the frequencies of

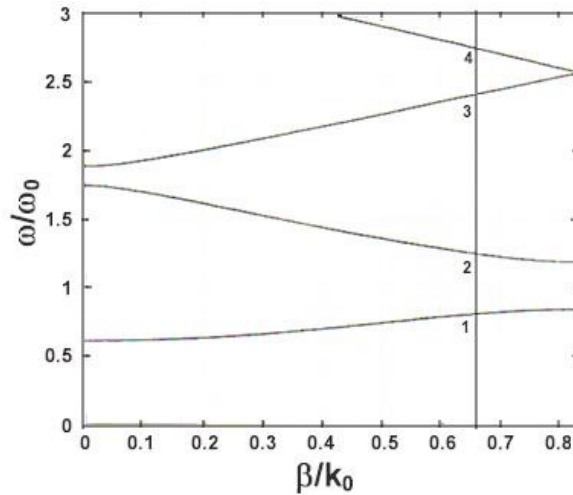


**Figure 1.** Dispersion relation  $\omega(\beta)$  for the case  $L = 0.6\lambda_0$ , and  $\omega_{p0} = 1.2\omega_0$ , where  $\lambda_0$  and  $\omega_0$  are the wavelength and angular frequency of an initial reference wave in free space.  $\beta/k_0 = -2\pi/k_0L + 1 = -0.667$ , the vertical line is at the mirror point  $\beta/k_0 = 0.667$  and its intersecting points with the dispersion curves determine the frequencies of the Floquet modes converted from the initial reference wave after interacting with the suddenly created periodic plasma.

all the Floquet modes at a given wavenumber. Shown in Figure 1 is an example of the dispersion curves for the case  $L = 0.6\lambda_0$ ,  $d = 0.2\lambda_0$ , and  $\omega_{p0} = 1.2\omega_0$  corresponding to the condition of the experiment presented in Section 4, where  $\lambda_0$  and  $f_0 = \omega_0/2\pi$  are the wavelength and initial frequency of a wave in the free space. The frequency gap between two adjacent branches of the dispersion curves forms a stop band, or a band gap, which is one of the characteristic features of periodic structures. Hence, for a given  $\beta L$ , there exists infinite number of Floquet modes oscillating at discrete frequencies  $\omega_j(\beta)$ . The vertical line in the figure is at the mirror point of  $\beta/k_0 = -2\pi/k_0L + 1 = -0.667$  and its intersecting points with the dispersion curves determine the frequencies of the Floquet modes converted from the initial reference wave  $(\omega_0, k_0)$  after interacting with this instantly created periodic plasma. Substitute  $k = k_j = \omega_j(\beta)/c$  into (10) and (12), and use (12) to replace the coefficients  $B, C$  and  $D$  in (10) in terms of  $A$ , the field distribution of the  $j$ th Floquet mode is obtained.

### 3.2. Wave Propagation in Suddenly Created Periodic Plasma

Propagation of a plane wave in such a medium, transition from the free space to a periodically structured plasma created instantly at  $t = 0$ , is analyzed in the following. The wave fields in  $t < 0$  are the same as those given in (2), which imposes the initial conditions (3a) and (3b). In  $t > 0$ , the wave has to satisfy the new dispersion relations governed by (13); thus, it is converted to a combination of infinite number of Floquet modes given by

$$\boldsymbol{\varepsilon}(z, t > 0) = \hat{\mathbf{x}}\Sigma A_{j\pm} \cos(k_0z \mp \omega_j t) \quad (14)$$

where the oscillation frequencies  $\omega_j(\beta)$  are the roots of (13),  $0 \leq -\beta = 2m\pi/L - k_0 \leq \pi/L$  and  $m$  is an integer. The amplitudes  $A_{j\pm}$  are imposed by the initial condition (3a) to be

$$\Sigma_{j=1}^{\infty} (A_{j+} + A_{j-}) = E_0 \quad (15)$$

From Faraday's Law  $\nabla \times \boldsymbol{\varepsilon} = -\mu_0 \partial_t \mathbf{h}$ , the corresponding wave magnetic field  $\mathbf{h}$  is obtained to be

$$\mathbf{h}(z, t > 0) = \hat{\mathbf{y}}\Sigma \pm (k_0/\mu_0\omega_j)A_{j\pm} \cos(k_0z \mp \omega_j t) + \mathbf{h}_w(z) \quad (16)$$

subjects to the initial condition  $h(z, t = 0) = (k_0/\mu_0\omega_0)E_0 \cos k_0z$ . Therefore, a wiggler magnetic field

$$\mathbf{h}_w(z) = \hat{\mathbf{y}}[(k_0/\mu_0\omega_0)E_0 - \Sigma \pm (k_0/\mu_0\omega_j)A_{j\pm}] \cos k_0z \quad (17)$$

is generated in the periodic plasma. With the aid of the initial condition  $\mathbf{j}(z, t = 0^+) = 0$ , the Ampere's law  $\nabla \times \mathbf{h} = \mathbf{j} + \varepsilon_0 \partial_t \boldsymbol{\varepsilon}$  at  $t = 0^+$  is applied to yield

$$\Sigma_j (\omega_j/\omega_0)(A_{j+} - A_{j-}) = E_0 \quad (18)$$

The relations (15) and (18) are combined to be

$$\Sigma_j [(1 - \omega_j/\omega_0)A_{j+} + (1 + \omega_j/\omega_0)A_{j-}] = 0 \quad (19)$$

In the limit of  $\ell \rightarrow 0$ , it approaches to uniform plasma situation; (13) has a root  $k_2 n_2 \cong \beta$ , which is the dispersion relation of the first frequency upshifted Floquet mode, i.e., in the  $j = 2$  branch; this root gives  $\omega_2 \cong (\omega_{p0}^2 + \beta^2 c^2)^{1/2}$ , approaching a uniform plasma dispersion relation presented in Section 2, where  $A_{2-} = [(1 - \omega_0/\omega_2)/(1 + \omega_0/\omega_2)]A_{2+}$  is derived. Thus a solution of (19), which matches the asymptotic solution, is

$$A_{j-} = [(1 - \omega_0/\omega_j)/(1 + \omega_0/\omega_j)]A_{j+} \quad (20)$$

which leads to

$$\Sigma_j [2/(1 + \omega_0/\omega_j)]A_{j+} = E_0 \quad (21)$$

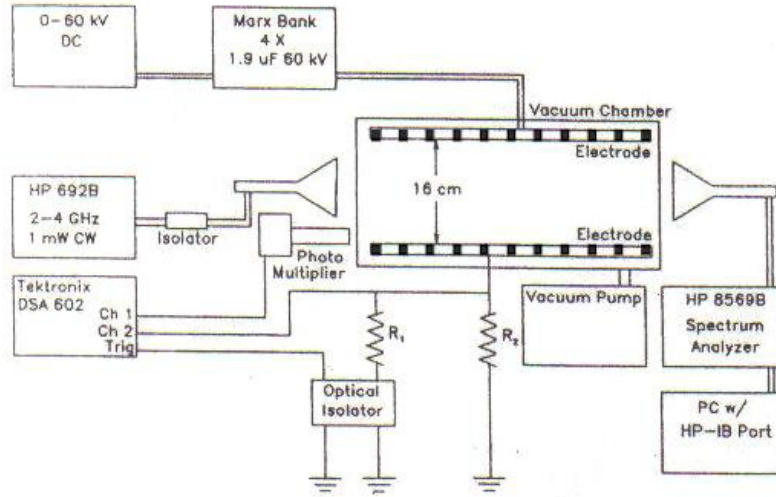


**Figure 2.** A schematic of the experimental setup.

## 4. EXPERIMENT AND NUMERICAL SIMULATION

### 4.1. Experimental Setup

A conducting plate is cut with 10 rectangular slots located evenly on the plate to make an electrode having a periodic pattern. A pair of such electrodes aligned parallelly with 16 cm separation is installed in a vacuum chamber where the background air pressure is about 1 torr. A Marx bank consisting of four simultaneously fired capacitors, each rated at  $1.9 \mu\text{F}$  and 60 kV, is connected to the electrodes. As the Marx bank is fired, periodically distributed plasma is created suddenly by the pulse discharge. Shown in Figure 2 is an overview of the experimental setup.

In the experiment, a CW microwave ( $\sim 1 \text{ mW}$ ) is launched into the vacuum chamber through an S-band horn antenna from one side. This incident signal is transmitted through this periodically structured plasma generated by the pulse discharge and is received by a horn antenna which is located at the other side of the chamber and connected to a spectrum analyzer for recording. Floquet modes described in Section 3.2. are expected to be produced, which form spectral peaks in the power spectrum. However, these modes generated in each discharge are short pulses and cannot be all recorded in one sweep of the spectrum analyzer. In other words, in each Marx bank discharge the spectrum analyzer stores a sample point of the power spectrum of the transmitted signal. After several hundred random Marx bank discharges, the stored sample points cover the entire power spectrum of the transmitted signal.

### 4.2. Experimental Result

Shown in Figure 3 is an experimentally recorded power spectrum of the incident (arrowed) and frequency downshifted signals [16]. The incident wave frequency is slightly below 3.1 GHz (indicated by an arrow) and the discharge voltage is 60 kV. The recorded spectrum shows only large downshifted components.

### 4.3. Numerical Simulation

We now solve (1) numerically for suddenly created periodic plasma characterized by (9). Following dimensionless parameters and variable are introduced

$$d/\lambda_0 \rightarrow d, \quad L/\lambda_0 \rightarrow L, \quad \omega_0 t \rightarrow t, \quad \omega_{p0}/\omega_0 \rightarrow \omega_{p0}, \quad \alpha = (\omega_0 \tau_r)^{-1} \quad \text{and} \quad \gamma = (\omega_0 \tau_d)^{-1}.$$

A finite difference time domain method [20] is used to solve the wave Equation (1) for computing the observed field  $E$  (in time) at a particular spatial location. This time series is subsequently Fast

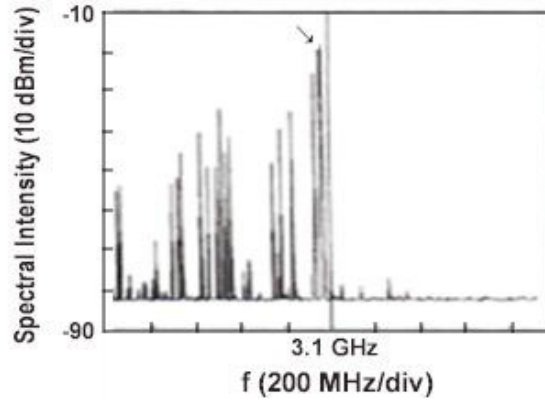


**Figure 3.** Experimentally recorded power spectrum of the incident (arrowed) and downshifted signals. The resolution bandwidth and the sweeping speed of the spectrum analyzer are 100 kHz and 10 s/div., respectively.

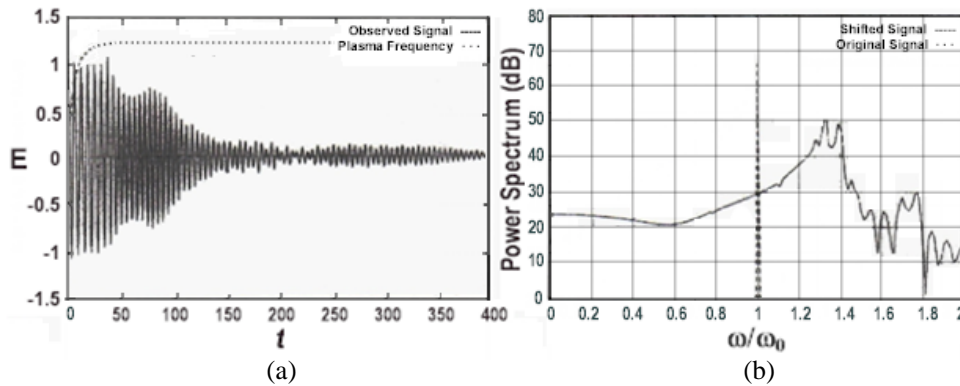


**Figure 4.** (a) Time dependence of the observed signal outside the plasma structure with  $N = 11$ ,  $L = 0.6$ ,  $d = 0.2$ ,  $\omega_{p0} = 1.2$ ,  $\alpha = 0.1$  and  $\gamma = 0$ , and (b) its power spectrum.

Fourier Transformed (FFT) and the power spectrum found by multiplying the time series' FFT by its complex conjugate.

Choose parameters used in the simulation closely corresponding to the experiment [16], thus,  $\omega_0 = 2\pi \times 3.1$  GHz,  $N = 11$ ,  $\omega_{p0} = 1.2$ ,  $\alpha = 0.1$ ,  $\gamma = 2 \times 10^{-3}$ ,  $L = 0.6$  and  $d = 0.2$ ; and the dispersion relation of the ideal structure (i.e.,  $N \rightarrow \infty$ ,  $\alpha \rightarrow \infty$ , and  $\gamma = 0$ ) presented in Figure 1 helps for justifying the simulation results on the spectra of frequency-shifted signals.

We first consider the  $\gamma = 0$  case (i.e., rapidly created plasma layers do not decay) to demonstrate the trapping effect of the periodic plasma layers. All the time plots display the observed signals, which are normalized to the amplitude of the incident signal. The spectral plots show the power spectra of the computed time series of the signals as observed inside (at  $z = 6$ ) or outside the plasmas (at  $z = 6.4$ ), using the incident wave as a reference. Presented in Figures 4(a) and 4(b) are the time dependence of the observed signal outside the plasma structure and its power spectrum, respectively. The time plot in Figure 4(a) shows that initially the observed signal keeps a large and near constant amplitude until the plasma density approaches a steady state overdense level (i.e.,  $\omega_{p0} > 1$ ). The signal then decays to a small level, implying no more signals transmit through the structure after the plasma density in layers reaches the steady state overdense level. This is realized that only frequency upshifted signals, which were generated during the short period of plasma creation, were not cutoff from propagation through the plasma layers. The power spectrum presented in Figure 4(b) also exhibits only an upshifted part, confirming the explanation.

However, the dispersion curves shown in Figure 1 indicate that a frequency downshifted signal

should also be generated during the short period of plasma creation. To show that the downshifted waves indeed exist and are trapped in the plasma, we move the observation point to be inside the periodic structure between two adjacent layers. The time function and power spectrum of the observed signal are presented in Figures 5(a) and 5(b), respectively. Figure 5(a) shows that the signal reaches a steady state level, rather than decaying to zero as that observed in Figure 4(a). This is an expected result as the downshifted wave is forever trapped to be the steady state signal after the escape of the upshifted waves. Indeed, the power spectrum presented in Figure 5(b) includes both up and downshifted lines. The downshifted spectrum has a sharper distribution and contains less spectral energy than that contained in the upshifted spectrum.

We now consider the experimental situation [16] that plasma decays at a rate  $\gamma = 2 \times 10^{-3}$ . The observation point is set outside the plasma structure. It is expected to detect both frequency upshifted and downshifted waves because the downshifted waves will not be trapped after the decay of the plasma. The time plot presented in Figure 6(a) shows that initially the observed signal is of large amplitude, decays to a small level, and later grows again. This can be explained as follows. Immediately after the plasma is created, the upshifted waves propagate out of the plasma. This explains the first part of the waveform with large amplitude. Once these waves are clear of the plasma, the signal amplitude drops as the downshifted waves remain trapped. However, as the plasma decays, the incident wave can again propagate through it to be converted and more and more of the downshifted waves can escape the trapping. These waves are responsible for the later rise in signal amplitude. The time delay between  $\omega_p$  falling below one and the rise in the signal in  $t > 50$  of Figure 6(a) can be explained by the

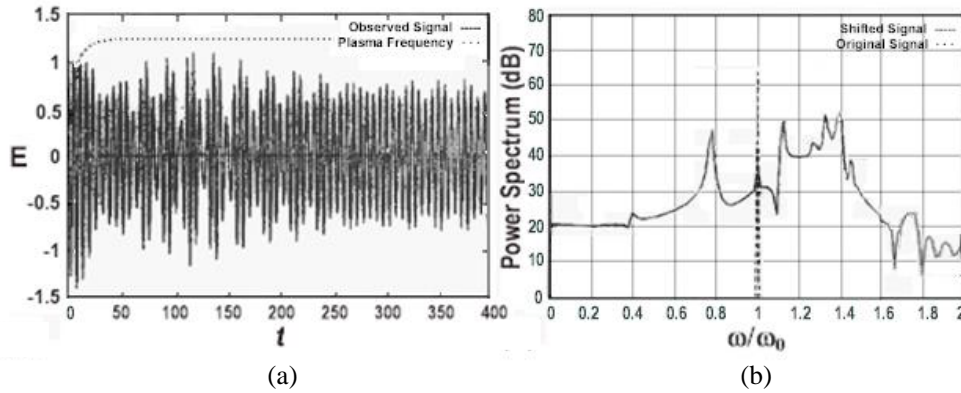


**Figure 5.** (a) Time dependence of the observed signal inside the plasma structure with  $N = 11$ ,  $L = 0.6$ ,  $d = 0.2$ ,  $\omega_{po} = 1.2$ ,  $\alpha = 0.1$  and  $\gamma = 0$ , and (b) its power spectrum.

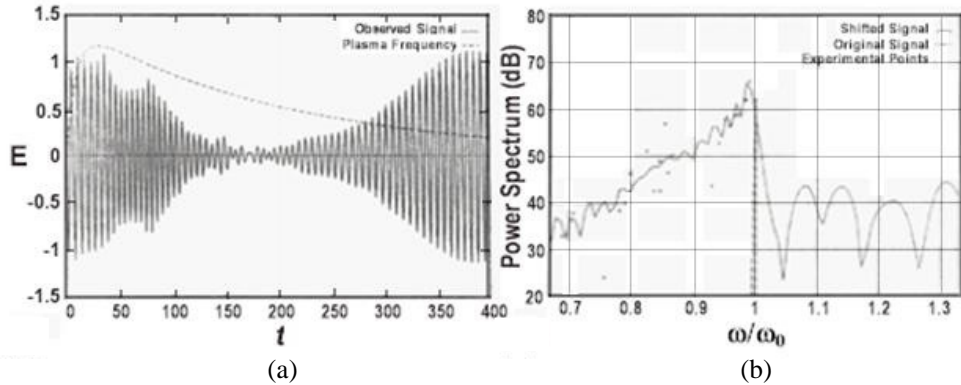


**Figure 6.** A simulation of the experiment with  $N = 11$ ,  $L = 0.6$ ,  $d = 0.2$ ,  $\omega_{po} = 1.2$ ,  $\alpha = 0.1$  and  $\gamma = 0.002$ . (a) Time dependence of the observed signal outside the plasma structure and (b) its power spectrum with prominent experimental points superimposed.

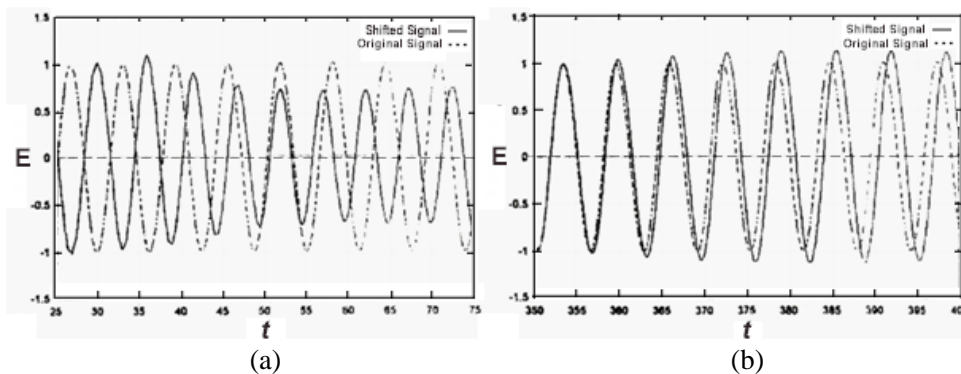


**Figure 7.** Comparison of the observed signal in Figure 6(a) with the original signal, (a) at early time showing upshifted frequency, and (b) at later time showing downshifted frequency.

finite propagation time of the waves from the plasma to the observation point. The power spectrum of this signal presented in Figure 6(b) reveals the usual upshifted peaks, but also a large downshifted part whose log power spectrum varies almost linearly with the frequency. The prominent experimental points extracted from Figure 3 are also presented in Figure 6(b) for comparison with the result of the numerical simulation. As shown, the simulation result matches well with that of the experiment.

A closer inspection on the detected signal reveals that the initial large wave packet contains only upshifted components and the latter only downshifted, as shown in Figures 7(a) and 7(b), respectively. Frequency downshifted waves are generated and trapped in the available period during the plasma growth and decay.

The trapped incident wave accumulates its energy during the finite growth period of the plasma and then emerges during the decaying period of the plasma. This leads to an enhancement of the spectral intensity and width of the frequency downshifted signal, a phenomenon which is not obvious from the band diagram presented in Figure 1.

With the aid of the simulation interpretation, the experiment demonstrates a unique approach to trap wave in an overdense periodic plasma. The finite growth and decay of suddenly created plasma broaden the spectrum of the frequency downshifted signals, but this plasma is able to generate more frequency downshifted waves and accumulate those waves.

## 5. SUMMARY

Applying Bloch's theorem to the boundary conditions, the dispersion relation of an EM wave propagating in a spatially periodic plasma medium is derived. It consists of infinite branches of dispersion curves, each one representing a Floquet mode and covering a frequency range as a pass band. The frequency gap between two adjacent branches of these dispersion curves forms a band gap as stop band. An interesting feature of the dispersion curves is that the pass bands extend to the region below the cutoff frequency ( $\omega_p$ ) of uniform plasma. It infers that a suddenly created periodic plasma can convert a pre-existing electromagnetic wave into both frequency upshifted and downshifted new waves. The numerical simulation shows that frequency downshifted waves are indeed generated and trapped in plasma. The plasma decay enables more frequency downshifted waves of increasing frequency (i.e., decreasing in the amount of frequency downshift) to be trapped; it results in a significant enhancement of the spectral width and intensity, explaining the experimental observation.

The wave impedance of the frequency downshifted mode is large in the free space region and small in the plasma layer, but it has the opposite distribution for the frequency upshifted modes [21]. This characteristic difference indicates that the trapped frequency downshifted waves are experience reduced collision damping in the plasma layer. On the other hand, the untrapped frequency upshifted waves undergo enhanced collision damping in the plasma layer. It provides a plausible explanation why only the frequency downshifted signals were detected convincingly in the experiments [16] with considerably enhanced spectral width and intensity while the frequency upshifted signals were not observed.

Trapping of waves in periodic dielectric media has been investigated extensively in the photonic research [22–24]. The mechanism of wave trapping is to have the wave frequency in the stop bands of the periodic dielectric medium. This trapping process has to overcome the difficulty of coupling radiation into the cavity surrounded by the cutoff structure (i.e., the periodic structure). On the other hand, this difficulty is not encountered in the time domain case as demonstrated experimentally. It is the periodic dielectric medium (plasma) suddenly created around the waves, rather than that wave has to penetrate into the cavity. Moreover, the trapped waves in the time domain case are distributed in the periodic structure and are the modes of the periodic structure.

## ACKNOWLEDGMENT

The author gratefully acknowledges fruitful discussions with Professor G. Schmidt of Stevens Institute of Technology. He also likes to thank Drs. James Faith and Joe Huang for their assistance in the numerical work. This work was supported by the Air Force Office of Scientific Research (AFOSR).

## REFERENCES

1. Morgenthaler, F., "Velocity modulation of electromagnetic waves," *IRE Trans. Microwave Theory Tech.*, Vol. 6, 167–172, 1958.
2. Felsen, L. B. and G. M. Whitman, "Wave propagation in time-varying media," *IEEE Trans. Antennas Propag.*, Vol. 18, 242–253, 1970.
3. Jiang, C. L., "Wave propagation and dipole radiation in a suddenly created plasma," *IEEE Trans. Antennas Propag.*, Vol. 231, 83–90, 1975.
4. Wilks, S. C., J. M. Dawson, and W. B. Mori, "Frequency up-conversion of electromagnetic radiation with use of an overdense plasma," *Phys. Rev. Lett.*, Vol. 61, 337–340, 1988.
5. Kuo, S. P., A. Ren, and J. Huang, "Generation of a frequency chirped pulse using phase velocity transitions in a rapidly created plasma," *Ultra Wideband EM Waves*, 129–136, H. L. Bertoni, Ed., Plenum Press, NY, 1993.
6. Rappaport, H. L. and C. D. Striffler, "Frequency up-conversion and time-dependent tunneling of electromagnetic radiation in step-ionized plasmas," *Phys. Plasmas*, Vol. 1, 780–784, 1994.
7. Yablonovitch, E., "Spectral broadening in the light transmitted through a rapidly growing plasma," *Phys. Rev. Lett.*, Vol. 31, 877–879, 1973.
8. Yablonovitch, E., "Self-phase modulation of light in a laser-breakdown plasma," *Phys. Rev. Lett.*, Vol. 32, 1101–1104, 1974.
9. Kuo, S. P., "Frequency up-conversion of microwave pulse in a rapidly growing plasma," *Phys. Rev. Lett.*, Vol. 65, No. 8, 1000–1003, 1990.
10. Joshi, C. J., C. E. Clayton, K. Marsh, D. B. Hopkins, A. Sessler, and D. Whittum, "Demonstration of the frequency upshifting of microwave radiation by rapid plasma creation," *IEEE Trans. Plasma Sci.*, Vol. 18, 814–818, 1990.
11. Kuo, S. P., Y. S. Zhang, and A. Ren, "Observation of frequency up-conversion in the propagation of a high power microwave pulse in a self-generated plasma," *Phys. Lett. A*, Vol. 150A, No. 2, 92–96, 1990.
12. Kuo, S. P. and A. Ren, "Frequency up-conversion of a high power microwave pulse propagating in a self-generated plasma," *J. Appl. Phys.*, Vol. 71, No. 11, 5376–5380, 1992.
13. Kuo, S. P. and A. Ren, "Experimental study of wave propagation through a rapidly created plasma," *IEEE Trans. Plasma Sci.*, Vol. 21, No. 1, 53–56, 1993.
14. Kuo, S. P., A. Ren, and G. Schmidt, "Frequency downshift in rapidly ionizing media," *Phys. Rev. E*, Vol. 49, No. 4, 3310–3315, 1994.
15. Ishimaru, A., *Electromagnetic Wave Propagation, Radiation, and Scattering*, Prentice Hall, Englewood Cliffs, NJ, 1991.

16. Faith, J., S. P. Kuo, and J. Huang, "Frequency downshifting and trapping of an electromagnetic wave by a rapidly created spatially periodic plasma," *Phys. Rev. E.*, Vol. 55, No. 2, 1843–1851, 1997.
17. Qi, L. and Z. Yang, "Modified plane wave method analysis of dielectric plasma photonic crystal," *Progress In Electromagnetics Research*, Vol. 91, 319–332, 2009.
18. Minin, I. V., O. V. Minin, Y. R. Triandaphilov, and V. V. Kotlyar, "Subwavelength diffractive photonic crystal lens," *Progress In Electromagnetics Research B*, Vol. 7, 257–264, 2008.
19. Blatt, F. J., *Physics of Electronic Conduction in Solids*, McGraw Hill, NY, 1970.
20. Press, W. H., S. A. Teukolsky, W. T. Vetterling, and B. P. Flannery, *Numerical Recipes: The Art of Scientific Computing*, 2nd edition, Cambridge University Press, New York, NY, 1992, ISBN: 0-521-43108-5.
21. Kuo, S. P. and J. Faith, "Interaction of an electromagnetic wave with a rapidly created spatially periodic plasma," *Phys. Rev. E*, Vol. 56, No. 2, 2143–2150, 1997.
22. Leung, K. M. and Y. F. Liu, "Full vector wave calculation of photonic band structures in face-centered-cubic dielectric media," *Phys. Rev. Lett.*, Vol. 65, No. 21, 2646–2649, 1990.
23. Yablonovitch, E., T. J. Gmitter, and K. M. Leung, "Photonic band structure: The face-centered-cubic case employing nonspherical atoms," *Phys. Rev. Lett.*, Vol. 67, 2295–2298, 1991.
24. Chen, J.-Y., J.-Y. Yeh, L.-W. Chen, Y.-G. Li, and C.-C. Wang, "Design and modeling for enhancement of light extraction in light-emitting diodes with archimedean lattice photonic crystals," *Progress In Electromagnetics Research B*, Vol. 11, 265–279, 2009.